Vibration Reduction in a Multimass Flexible Rotor Using a Midspan Magnetic Damper

P. E. Allaire, Professor
M. E. F. Kasarda, Research Associate
R. R. Humphris, Research Professor
D. W. Lewis, Professor

Department of Mechanical and Aerospace Engineering
University of Virginia
Charlottesville, VA 22901 USA

Summary

The purpose of this study is to investigate the effects of a magnetic damper on a multimass rotor. A small three mass rotor which would simulate the dynamics of a centrally mounted steam turbine or compressor was built and a magnetic damper placed near the rotor midspan. The magnetic damper was constructed of four separate radially arranged silicon iron magnets with coil windings. A proportional and derivative control circuit was employed to control the damper. The rotor was run at speeds from 0 to 10,000 rpm, through three natural rotor-bearing-support system resonances.

Introduction

Rotating machines with long thin shafts often have vibration problems. Modern steam turbines, compressor, and gas turbines operate above the first critical speed in many cases. Large clearances must be maintained in the seals to avoid contact during running through the critical speed. Some high speed machines even operate above two or more critical speeds. The trend is to higher speeds and thinner shafts to improve operating efficiencies so that vibration problems will continue to be present.

A damper placed at the center of such machines could control the high levels of vibration. Until recent years, no damper could operate in the working fluid of the rotating machine because the temperature was too high (steam turbine) or the gas would become contaminated with the oil used in the damper (compressor) unless complicated seals were used.

---

*Partial support for this work was obtained from the U.S. Army Research Office and the Center for Innovative Technology of the Commonwealth of Virginia.

Magnetic dampers can now be used in industrial machines for vibration reduction. Magnetic bearings are being employed in compressors such as natural gas pipeline compressors. Many other papers are available in the literature on applications or research related to magnetic bearings used for support of rotating machines. Due to length restrictions, these will not be discussed in this paper except when they relate directly to the damper employed in this study.

Magnetic dampers have been reported in the literature in only a few cases. Nikolajsen et al. [1] described a magnetic damper used to control vibrations in a long transmission shaft. This pioneering work discussed both the design of the damper and its optimum location along the shaft. Another paper by Gondhalekar et al. [2] gave further developments in this project.

Burrows and Sahinkaya [3,4] applied an electromagnetic damper to a laboratory rotor supported in fluid film bearings. They considered the effects of employing a limited number of measurement sites on controller performance. Vibration reduction of 90% was obtained for the first mode. Wai and Morel [5] used a large midspan damper to control a single mass test rig.

Allaire, et al. [6] presented a paper on the use of a centrally mounted magnetic damper. An experimental test rig was set up with a long thin shaft and several masses to represent a flexible shaft machine. A dramatic reduction in vibration amplitude was obtained at the rotor center with the damper on. Kasarda, et al. [7] reported further work with that damper in controlling vibrations through the rotor first mode. The magnetic damper was placed in three locations: near the midspan, near one end disk, and close to the bearing. With typical control parameter settings, the midspan location reduced the first mode vibration 82%, the disk location reduced it 75% and the bearing location attained a 74% reduction. Magnetic damper stiffness and damping values used to obtain these reductions were only a few percent of the bearing stiffness and damping values. A theoretical model of both the rotor and the damper was developed and compared to the measured results with good agreement.

Some aspects of the control algorithms used in the works [6,7] were discussed by Humphris et al. [8]. The same magnetic bearing/damper

configuration was employed in other papers [9,10,11]. All of the above work was carried out with an analog controller as described in [8]. Recently a digital controller has also been developed for the magnetic bearing/damper [12] and successfully rotor test rig runs carried out.

The purpose of this paper is to report on some new magnetic damper research. The damper magnetic component remained the same as [6,7] but a new electronic controller was employed. The initial controller had some amplifiers which would saturate under high speed and amplitude of vibration conditions. Thus it did not operate well above a speed of about 4,000 rpm. The transfer function for the new controller is given in Appendix A. It allowed for damper test rig operation up to 10,000 rpm as well as more independent variation of the damper proportional and derivative gains.

Magnetic Damper

The magnetic damper employed in this study consisted of four electromagnets located radially around the rotor. Figure 1 illustrates the geometry as employed in this study [6,7,8]. It is an active damper, as compared to a passive damper, because the electromagnets have currents continually adjusted by an automatic feedback control circuit. The feedback signal is provided by induction probes which sense the displacement of the shaft [8]. A damper differs from a bearing in that it does not support a steady state load in any direction. Rather, it provides damping, and possibly stiffness, in response to shaft lateral vibrations.

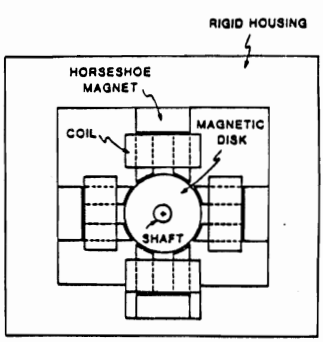

Fig. 1 Magnetic Damper Model

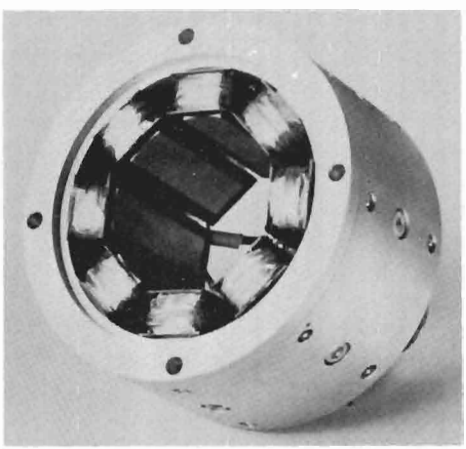

Fig. 2 Pump Bearing

Figure 2 shows a magnetic bearing/damper suitable for use in a rotating machine. It is employed in a canned motor pump at the University of Virginia. The prototype damper shown in Figure 1 used in this study is an older version which was available for this study.

The four electromagnets were located radially around a laminated ferromagnetic disk attached to the rotor shaft. Each magnet core consisted of a silicon-iron horseshoe with pole faces cut to a diameter of 60.5 mm (2.38 inches). The radial clearance was 1.0 mm (0.040 inches). Each leg of the coil was wound with 920 turns of wire. The disk provided a continuous flux path between the magnets and the rotor with a minimum of eddy current losses. All steady state bias currents in the four magnets were the same.

Two position sensing eddy current probes of standard commercial design were placed in the horizontal and vertical directions. They were located axially near the damper for feedback control. Various tests were conducted to insure that there was no coupling between the probes and the magnetic fields from the magnets.

The dynamic properties of the damper are very important to the level of vibration control of the rotor. A discussion of these properties is given in [7]. The two basic control gains in the damper were the proportional gain, denoted as K_g, and the derivative gain, denoted as K_r. It is shown in [7] that the proportional gain is directly related to the effective stiffness coefficient of the damper while the derivative gain is related to the effective damping coefficient. Other studies with this bearing/damper have verified that the stiffness is linear with K_g and that the damping is linear with K_r [8].

The three mass laboratory rotor, shown in Figure 3, was assembled with a 19.0 mm (0.75 inch) shaft supported in conventional sleeve bearings with a bearing span of 660.4 mm (26.0 inches). The total rotor length and weight, including the laminated magnetic disk, was 762 mm (30.0 inches) and 107.2 N (24.1 lb), respectively. Three steel disks were placed four inches apart at the center of the shaft leaving 190.5 mm (7.5 inches) between each outboard disk and the closest support bearing. Each of these three disks was 139.7 mm (5.5 inches) in diameter, 25.4 mm (1.0 inch) in thickness, and weighed 28.48 N (6.4 lbs).

Experimental and Analytical Results vs. Damping

The rotor was operated through a speed range of 0 to 10,000 rpm as shown in Figure 4. Only the vertical probe measurements on the rotor at the

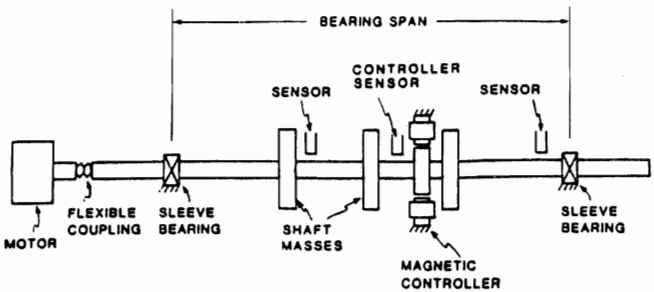

Fig. 3 Schematic of 3-Mass Rotor with Magnetic Damper at Midspan (Not to Scale)

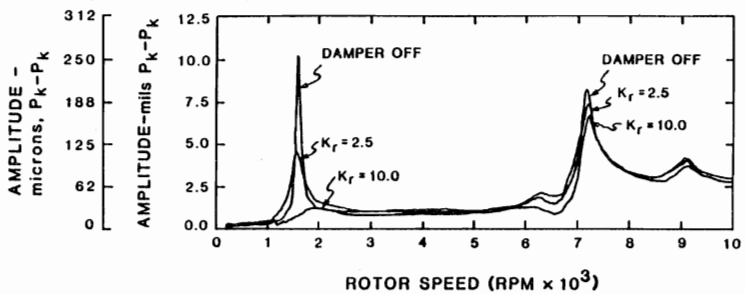

Fig. 4 Experimental Response of 3-Mass Rotor when the Damper is at the Midspan (Effect of Increasing Rate Gain (K_r)) - Response of Vertical Disk One Probe (K_g = 0.0)

left end disk are shown for simplicity. With the damper off, three critical speeds were observed in the rotor. These were at approximately 1600, 7200, and 9000 rpm. An undamped critical speed analysis predicted critical speeds at 1641, 6176, 8465, 8879, and 16004 rpm. The first two matched the observed first and second critical fairly well. The third critical calculated at 8465 rpm was a well damped cantilever mode of the motor which did not appear in the measurements. The undamped fourth critical speed at 8879 rpm corresponded to a pedestal mode measured at 9000 rpm. It was modeled with a support flexibility in the analytical model for the critical speeds. The 16004 rpm mode was above the running speed range.

Bearing properties for this test rig were estimated by comparison with analysis. The bearing stiffness was approximately 2,100,000 N/m (12,000 lb/in) and the bearing damping was estimated at 1100 N-s/m (6.4 lb-s/in).

Damper properties were obtained by the method described in Appendix B. In the speed range of the first critical speed, approximately 1600 rpm, the damper had an estimated stiffness of -9,000 N/m (-50 lb/in) for a proportional gain K_g = 0.0 and a damping of 31 N-s/m (0.18 lb-s/in) for a rate gain K_r = 2.5. An increase in the rate gain setting to K_r = 10 corresponded to a damping of 66 N-s/m (0.38 lb-s/in).

At 1600 rpm, the damper had the effect of reducing the amplitude at the probe from 260 microns (10 mils) pk-pk to 120 microns (4.5 mils) pk-pk with K_r = 2.5. A slight decrease in the critical speed was due to the negative stiffness of the damper. At K_r = 10, the amplitude was reduced further to approximately 32 microns (1.3 mils) pk-pk. This was an overall reduction of 88% over the case with no damper.

For the second rotor critical speed at 7200 rpm, the damper had much less effect. The damper stiffness was estimated at 28,000 N/m (160 lb/in). The estimated damping was 30 N-s/m (0.17 lb-s/in) at K_r = 2.5 and 5.3 N-s/m (0.03 lb-s/in) at K_r = 10. With no damper, the amplitude was 210 microns (8.5 mils) pk-pk. With the damper at K_r = 10, the amplitude was 180 microns (7.4 mils) pk-pk. This was only a 13% overall decrease.

The pedestal mode at 9,000 rpm showed a small reduction as well. At K_r = 10, the overall reduction was about 18%.

An analytical unbalance reponse computer run was carried out for each of the speed ranges near critical speeds. Figure 5 shows the results obtained near the first critical. The overall reduction in amplitude is 81% for K_r = 10 as compared with the measured reduction of 88%. Results

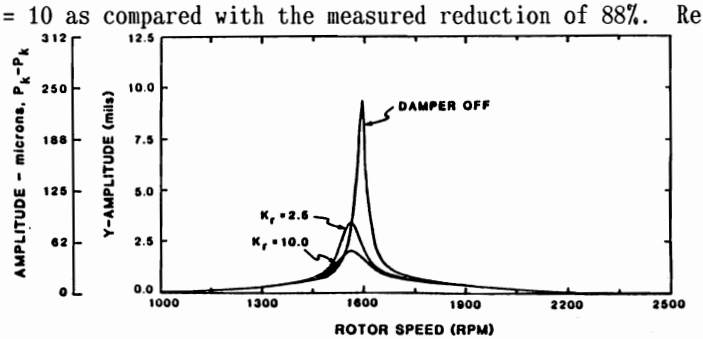

Fig. 5 Forced response predictions when Damper is at the Midspan (Effect of Increasing Rate Gain (K_r)) - First Mode Response at Vertical Disk One Probe (K_g = 0.0)

for other speed ranges were also obtained but the plots are not shown here because of space limitations. Generally the agreement was good when the estimated damper stiffness and damping coefficients were employed.

Experimental Results Vs. Stiffness

The effect of proportional gain K_g for the damper at the midspan is shown in Figure 6. The estimated damper stiffness with K_g = 2.5 was 140,000 N/m (800 lb/in). No estimate of the stiffness was made for K_g = 10. The rate gain was held at K_r = 10.

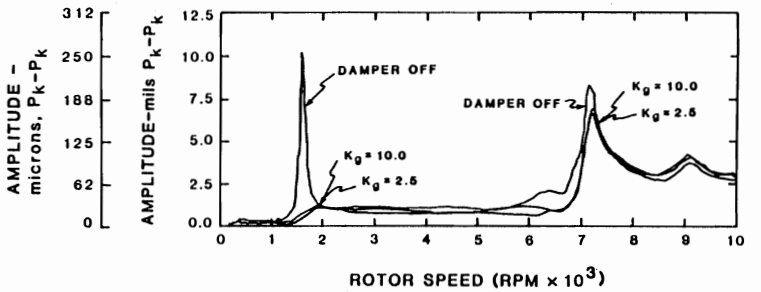

Fig. 6 Experimental Response of 3-Mass Rotor when the Damper is at the Midspan (Effect of Increasing Proportional Gain (K_g)) Response at Vertical Disk One Probe (K_r = 10.0)

The measured result for both K_g cases is overdamped so the exact frequency is difficult to determine. There appears to be approximately a 50 rpm increase for both runs. There is little effect on either the second critical speed or the pedestal mode.

Conclusions

Experimental and analytic studies have been carried out on the forced response characteristics of a three mass rotor with a midspan magnetic damper. Vibration reductions were observed near the left end disk in all cases to be consistent. With an increase in damping as discussed earlier in the paper, the amplitude of vibration was reduced by 88%, 13%, and 8% for the three critical speeds of the rotor. Small shifts in frequency were found with changes in damper stiffness, at the highest damping value.

In all cases presented in this paper, the damper was located near the midspan of the rotor. The first mode of vibration was the largest at the midspan so it was reasonable to expect the largest reduction in amplitude for that mode. The second mode of vibration had a node point near the

midspan. Thus it was expected that the vibration reduction would not be as good. Similarly, in the pedestal mode, the shaft and rotor base are moving together. Thus the damper, fixed to the base, did not have much effect on that mode. Other damper locations will be discussed in future papers.

References

1. Nikolajsen, J., Holmes, R., and Gondhalekar, V., "Investigation of an Electromagnetic Damper for Vibration Control of a Transmission Shaft," IMechE, 1979, pp. 331-336.

2. Gondhalekar, V. and Holmes, R., "Design of an Electromagnetic Bearing for the Vibration Control of a Flexible Transmission Shaft," Rotor Dynamics Instability Problems in High Performance Turbomachinery, Texas A&M University, May 1984.

3. Sahinkaya, M. N., and Burrow, C. R., "Control of Stability and the Synchronous Vibration of a Flexible Rotor Supported on Oil-Film Bearings," ASME Journal of Dynamic Systems, Measurement and Controls, Vol. 107, 1985, pp. 139-144.

4. Burrows, C. R., Sahinkaya, M. N., and Clements, S., "Electromagnetic Control of Oil-Film Supported Rotors Using Sparse Measurements," Rotating Machinery Dynamics, ASME Publication, September 27-30, 1987, pp. 127-132.

5. Wai, C. C. H., and Morel, J., "Application of an Active Magnetic Bearing for Vibration Control Near Critical Speeds in Large Rotating Machines," Rotating Machinery Dynamics, ASME Publication, September 27-30, 1987, pp. 151-158.

6. Allaire, P. E., Humphris, R. R., Kasarda, M. E. F., and Koolman, M. I., "Magnetic Bearing/Damper Effects on Unbalance Response of Flexible Rotors," Proc. AIAA Conference, Philadelphia, PA, August 10-14, 1987.

7. Kasarda, M. E. F., Allaire, P. E., Humphris, R. R., and Barrett, L. E., "A Magnetic Damper For First Mode Vibration Reduction in Multimass Flexible Rotors," Workshop on Rotordynamic Problems in High-Performance Turbomachinery, Texas A&M University, May 1988.

8. Humphris, R. R., Kelm, R. D., Lewis, D. W., and Allaire, P. E., "The Effect of Control Algorithms on Magnetic Journal Bearing Properties," Journal of Engineering for Gas Turbines and Power, Trans. ASME, Vol. 108, No. 4, October 1986, pp. 624-632.

9. Allaire, P. E., Lewis, D. W., and Knight, J. D., "Active Vibration Control of a Single Mass Rotor on Flexible Supports," Journal of the Franklin Institute, Vol. 315, 1983, pp. 211-222.

10. Allaire, P. E., Humphris, R. R., and Barrett, L. E., "Critical Speeds and Unbalance Response of a Flexible Rotor in Magnetic Bearings," Proc. of European Turbomachinery Symposium, October 27-28, 1986.

11. Allaire, P. E., Humphris, R. R., and Imlach, J., "Vibration Control of Flexible Rotors with Magnetic Bearing Supports," AFOSR/ARO Conference, Nonlinear Vibrations, Stability, and Dynamics of Structures and Mechanisms, Virginia Tech, Blacksburg, Virginia, March 23-25, 1987.

12. Keith, F. J., Williams, R. D., Allaire, P. E., and Schafer, R. M., "Digital Control of Magnetic Bearings Supporting a Multimass Flexible Rotor," Presented at NASA Conference on Magnetic Suspension Technology, NASA Langley, February 2-4, 1988.

Appendix A - Controller For Active Magnetic Damper

A feedback control diagram of the controller is given in Figure 7. The controller transfer function is

$$G(s) = - K_p\ (0.1\ K_t) \left[\frac{sR_1CK_r}{(1+RCs)(1+R_1C_1s)} \right] \left(\frac{1}{1+\tau s}\right)$$

The nomenclature is the same as that in earlier papers.

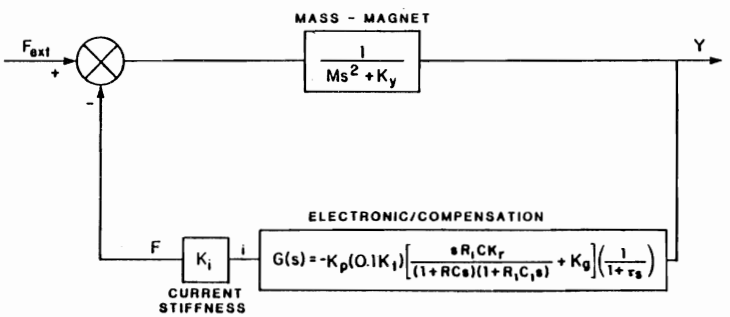

Fig. 7 Diagram of Magnetic Damper System

Appendix B - Determination of Damper Dynamic Properties

Damping and stiffness characteristics of the magnetic damper for various controller settings of proportional gain (K_g) and rate gain (K_r) were determined experimentally by examining the vibration characteristics of a single mass rotor as shown in [7]. The single mass rotor was

intentionally unbalanced and the effect of the electromagnetic damper (with various control settings) was compared to an analtyical model of the rotor-bearing system.

The effective stiffness of the damper is determined by the proportional gain (K_g) setting only. The effective damping of the magnetic damper is determined by the rate gain (K_r) setting.

A rotor model of the single mass rotor was established including support bearing characteristics, shaft bow, and unbalance in the rotor. The support bearings had a vertical stiffness of 4,030,000 N/m (23,000 lb/in) and a vertical damping of 10,000 N-sec/m (57 lb-sec/in). This model was used in a forced response program and the predicted response was compared to experimentally measured rotor response. Various values of stiffness and damping were added to the rotor model at the electromagnetic damper location until predicted response (i.e. frequency and amplitude of the first mode response) matched the experimental rotor response to within approximately 5%.